Supplementary Information

Polymorphism and Solid-Solid Phase Transitions of Hydrogen Bonded 2-adamantanol and 2-methyl-2-adamantanol Compounds

Alejandro Salvatori,[a] Philippe Negrier,[b] Stephane Massip[b], Antonio Muñoz-Duque[a], Pol Lloveras[a], Maria Barrio[a] and Josep-Lluís Tamarit[a,*]

[a] Grup de Caracterització de Materials, Departament de Física and Barcelona Research Center in Multiscale Science and Engineering, Universitat Politècnica de Catalunya,EEBE, Campus Diagonal-Besos, Av. Eduard Maristany 10-14, 08019 Barcelona, Catalonia

[b] Université de Bordeaux, Laboratoire d'Ondes et Matière d'Aquitaine, UMR 5798, F-33400 Talence, France

Table S1. Results from the Rietveld refinement for phase II of 2-adamantanol ($C_{10}H_{16}O$).

Chemical Formula	$C_{10}H_{16}O$
M / g·mol^{-1}	152.23
Phase	II
2θ-Angular Range	7-80
Space group	*C2/m*
a /Å	11.716(2)
b / Å	20.381(8)
c / Å	11.709(7)
α / º	90
β / º	109.58(3)
γ / º	90
V/Z / Å^3	2634(2)
Z (Z')	12(2)
Temperature	330K
D_x / g·cm^{-3}	1.152
Radiation type: X-Ray, λ	λ=1.540562Å
2θ-shift (zero correction)	0.0253 ± 0.0002
Profile Parameter, Na	0.184± 0.005
Reliability Parameters	
R_{wp}	4.98%
R_p	3.57%
Peak width parameters	
U	0.213 ± 0.031
V	-0.0762± 0.013
W	0.0185± 0.0014
Overall isotropic temperature factor, U / Å^2	0.1576± 0.002
Preferred Orientation	

(March Dollase function)[1]	
a*	-0.1536 ± 0.0048
b*	-0.8033± 0.0034
c*	0.575± 0.005
R0	1.607± 0.023
CCCD	2152769

Table S2. Hirshfeld surface volume (V), surface area (A), globularity (G) and asphericity (A), solid to plastic phase transition temperatures (T_{II-I}) and melting temperatures (T_{I-L}), and ratio between them (T_{II-I}/T_{I-L}) at normal pressure for some adamantane derivatives (short name identifies the compound in **Figure S5**). For compounds without plastic phase, the non-existing solid to plastic phase transition temperature is considered equal to the melting temperature. Short names in italic indicate the existence of the hydrogen bonds in the low-temperature ordered phase and in bold those calculated in this work. Details of the values can be found in reference [2].

Compound		Short Name	V/Å^3	A / Å^2	G	A	T_{II-I} /K	T_{I-L} /K	T_{II-I}/ T_{I-L}
Adamantane		A	192.3	178.03	0.905	0	208.6	543.2	0.384
1-fluoroadamantane		1FA	198.43	182.71	0.9	0.002	226	525	0.430
1-chloroadamantane		1ClA	220.23	196.7	0.897	0.018	248.6	439.7	0.565
1-bromoadamantane		1BrA	225.72	200.93	0.892	0.026	309.9	391.8	0.791
1-adamantanol		*1OA*	211.33	190.83	0.899	0.004	357.1	552.9	0.646
1,3-dibromoadamantane		13DBrA	260.75	224.15	0.881	0.023	382.1	382.1	1
1,3-dimethyladamantane		13DMA	249.27	218.77	0.876	0.019	222.6	246.8	0.902
1,3-adamantanediol		*13DOHA*	219.55	200.25	0.879	0.005	450.3	588.9	0.765
2-chloroadamantane		2ClA	217.97	194.64	0.900	0.014	240.9	467.5	0.515
2-bromoadamantane		2BrA	224.06	200.11	0.892	0.016	277.9	413.4	0.672
2-adamantanone		*2OA*					221.0	557.5	0.396
Ordered stable orthorhombic 190K			194.68	181.98	0.893	0.003			
Disordered metastable monoclinic 190K		*Molecule 1*	197.72	184.10	0.892	0.002			
		Molecule 2	197.71	183.89	0.0892	0.002			
		Molecule 3	197.83	184.10	0.892	0.001			
1-adamantane-methanol[b]		*1MOA*					389.5	389.5	1
100K		*Molecule 1*	240.35	208.42	0.897	0.019			
		Molecule 2	238.22	210.4	0.883	0.017			
		Molecule 3	240.27	208.58	0.896	0.020			
275K	*Direction 1*	*Molecule 1*	240.81	209.26	0.894	0.026			
		Molecule 2	241.47	210.36	0.891	0.023			
		Molecule 3	241.93	210.81	0.891	0.023			
	Direction 2	*Molecule 1*	240.85	209.23	0.896	0.026			
		Molecule 2	241.53	210.59	0.891	0.023			
		Molecule 3	241.82	210.57	0.891	0.023			
2-adamantanol[a]		*2-Aol*					389.3	567.3	0.686
150K		*Molecule 1*	201.97	184.69	0.901	0.003			
		Molecule 2	200.95	184.62	0.899	0.003			
		Molecule 3	205.99	186.49	0.904	0.002			

293K	*Direction 1*	*Molecule 1*	209.41	187.37	0.910	0.002			
		Molecule 2	209.20	187.64	0.908	0.003			
		Molecule 3	212.75	189.12	0.911	0.002			
	Direction 2	*Molecule 1*	209.18	186.75	0.912	0.002			
		Molecule 2	209.20	187.94	0.908	0.003			
		Molecule 3	212.75	188.98	0.912	0.002			
2-methyl-2-adamantanol[a]		*2-M-Aol*					367.5	488.8	0.752
293K		*Molecule 1*	226.29	201.29	0.892	0.015			
		Molecule 2	226.58	201.30	0.893	0.014			

a Values of V and A of the Hirshfeld analysis were calculated for the different configurations (3 for 2-Aol and 2 for 2-M-Aol) due to the presence of independent molecules, within the low-temperature monoclinic phases. For the other adamantane derivatives compiled within the table details can be obtained from ref [2].
b. Values for 1-adamantane-methanol has been also quoted for all the independent molecules in both phases unlike values gathered in ref. [2] where only average values were provided.

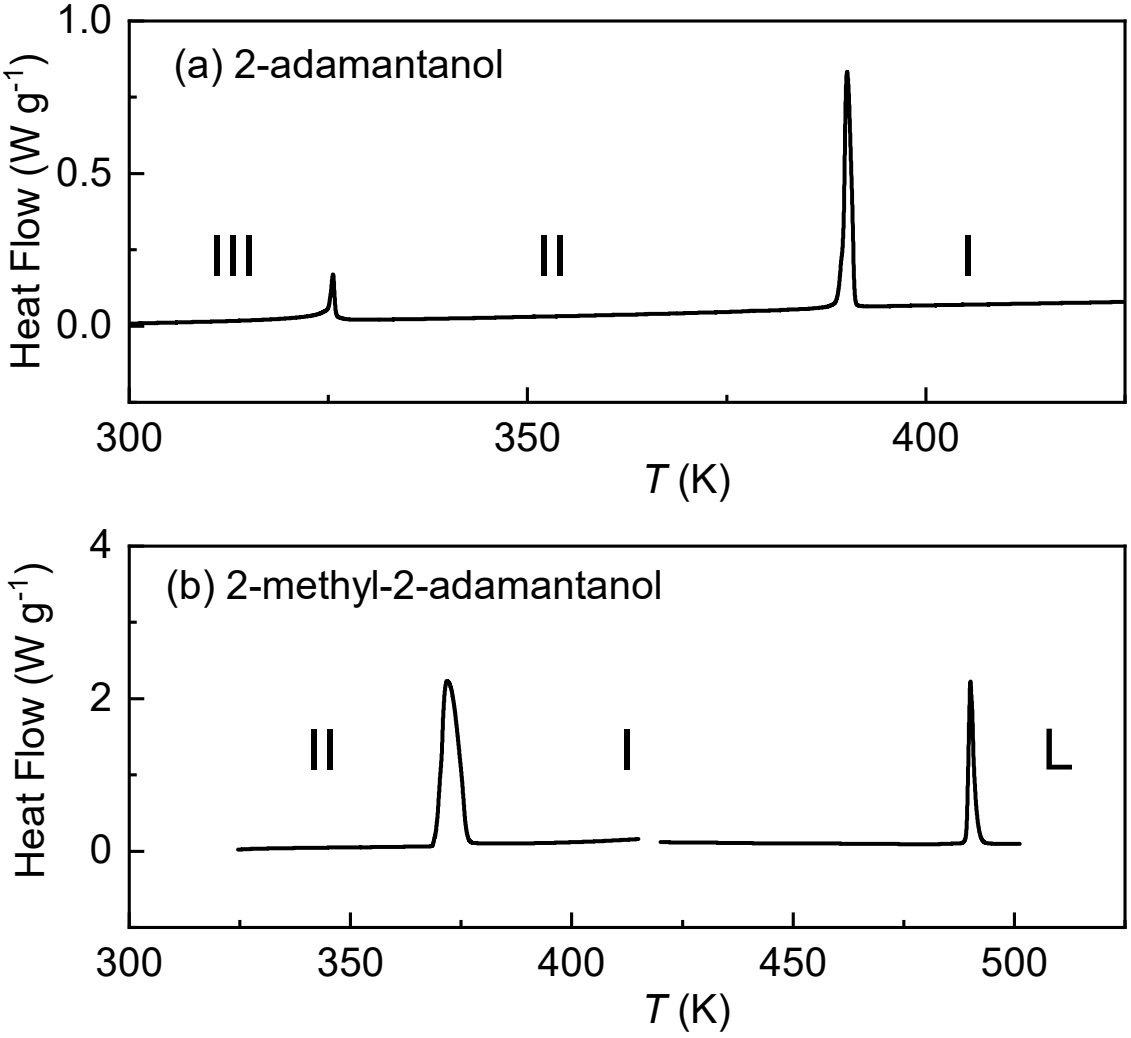

Figure S1. Differential scanning measurements on heating for the 2-adamantanol (top panel) and 2-methyl-2-adamantanol (bottom panel). The I to L melting for 2-adamantanol was not measured due to the high-vapor pressure at high temperature.

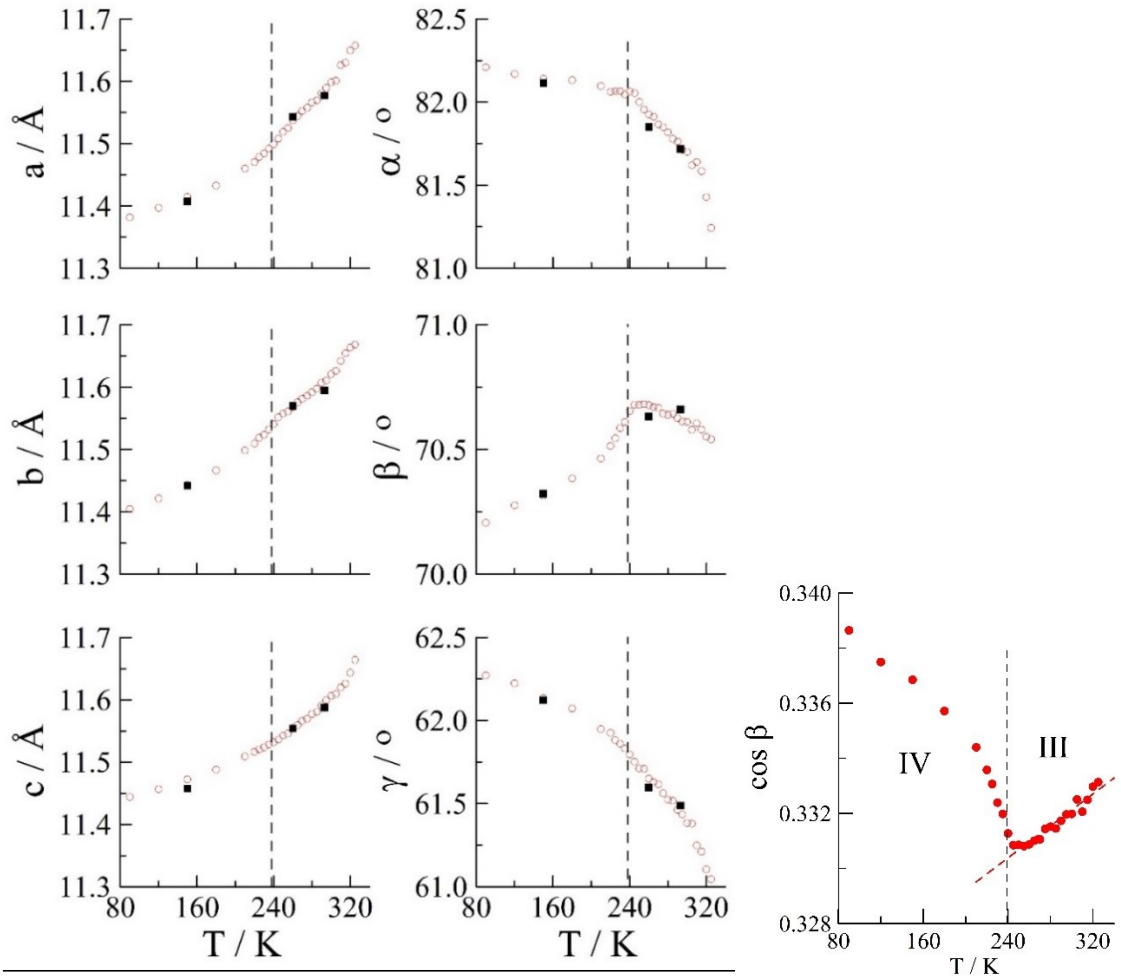

Figure S2. Lattice parameters as a function of temperature for phases IV and III of 2-adamantanol. Vertical dashed line indicates the transition temperature reported from adiabatic calorimetry [3]. Empty symbols correspond to X-ray powder diffraction and full symbols to single-crystal X-ray diffraction. Right panel shows $\boldsymbol{cos\beta}$ (red points) obtained from X-ray powder diffraction and the linear fit (red dashed line) of the values for phase III used as a "base line" for the definition of the order parameter.

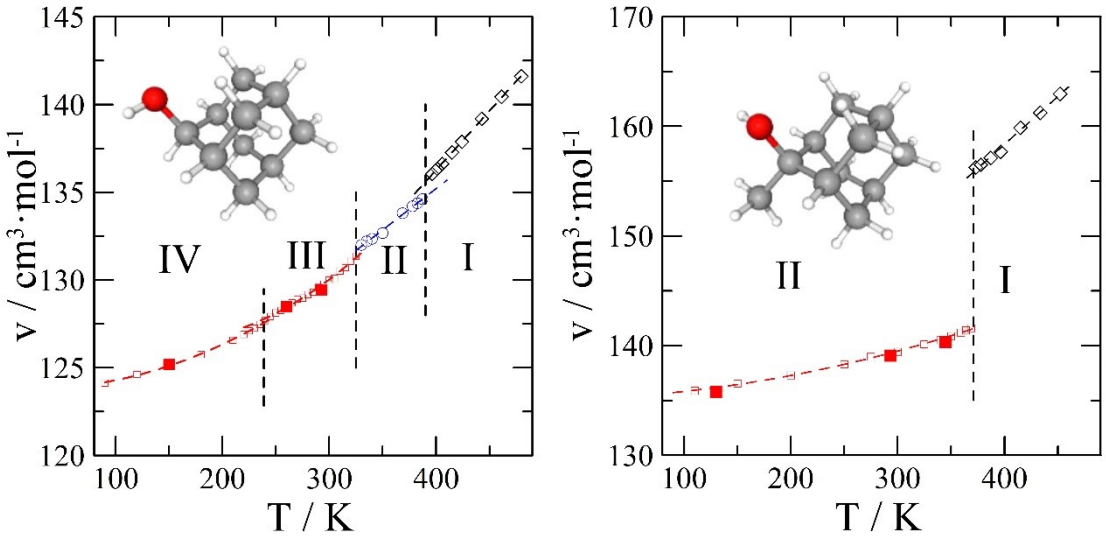

Figure S3. Molar volume for phases IV (empty and full red squares), III (empty and full red squares), II (empty blue circles) and I (empty black diamonds) of 2-adamantanol (left panel) and phases II (empty and full red squares) and I (empty black diamonds) of 2-methyl-2adamantanol (right panel) as a function of temperature. Empty symbols correspond to X-ray powder diffraction and full symbols to single-crystal X-ray diffraction. Vertical dashed lines correspond to the transition temperatures from adiabatic calorimetry [3, 4].

Structural relation between phase III and phase II of 2-adamantanol

The structure, space group $P\bar{1}$ (Z=6, Z'=3), of phase III at 293 K, determined by means of sing-crystal X-ray diffraction, is transformed to a pseudo-monoclinic P1 structure, through:

$$\begin{pmatrix} -1 & 0 & 0 \\ 1 & -2 & 0 \\ 0 & 0 & 1 \end{pmatrix}$$

$P\bar{1}$ (Z=6, Z'=3) (**Figure S3a**, left panel)

a=11.577 Å, b=11.5948 Å, c=11.5876 Å, α=81.718°, β=70.661°, γ=61.489°

Pseudo-Monoclinic, $P1$: (Z=12, Z'=12) (**Figure S3a**, right panel)

a=11.577 Å, b=20.3836 Å, c=11.5876 Å, α=88.613°(~90°), β=109.339°, γ=91.428°(~90°)

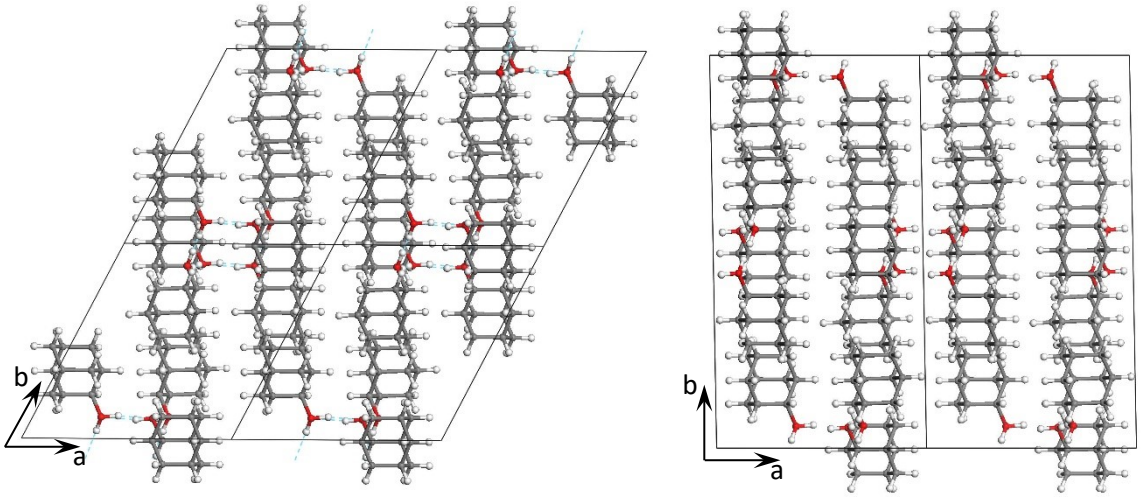

Figure S4a. Structure of phase III ($P\bar{1}$, Z=6, Z'=3) (left panel) and structure of phase III according to a pseudo-Monoclinic $P1$ space group (Z=12, Z'=12) (right panel)

From X-ray powder diffraction at 330 K; The Pawley profile-fitting procedure minimizing the R-factor (R_{wp}), gives C2/m space group with a=11.7071 Å, b=20.3477 Å, c= 11.6794 Å, α=90°, β=109.665°, γ=90°, to be compared with the pseudo-monoclinic P1 structure previously derived from phase III). In this solution, the number of molecules in the unit cell are now Z=12=8+4, and the number of independent molecules is reduced to Z'=1+1/2=1.5. The structure of phase II corresponds to 2 of the molecules of the pseudo-monoclinic P1 solution (see Figure S3b).

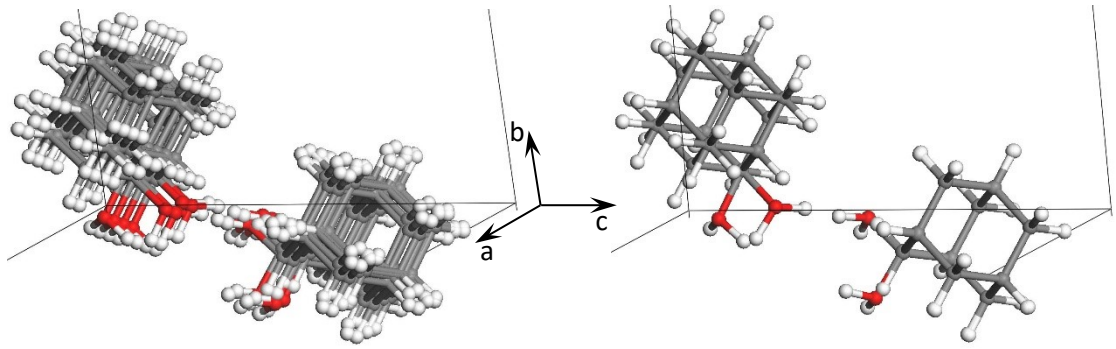

Figure S4b. Reconstructed structure with the C2/m applied symmetries (left panel) and the same structure wiping out the duplicated molecules.

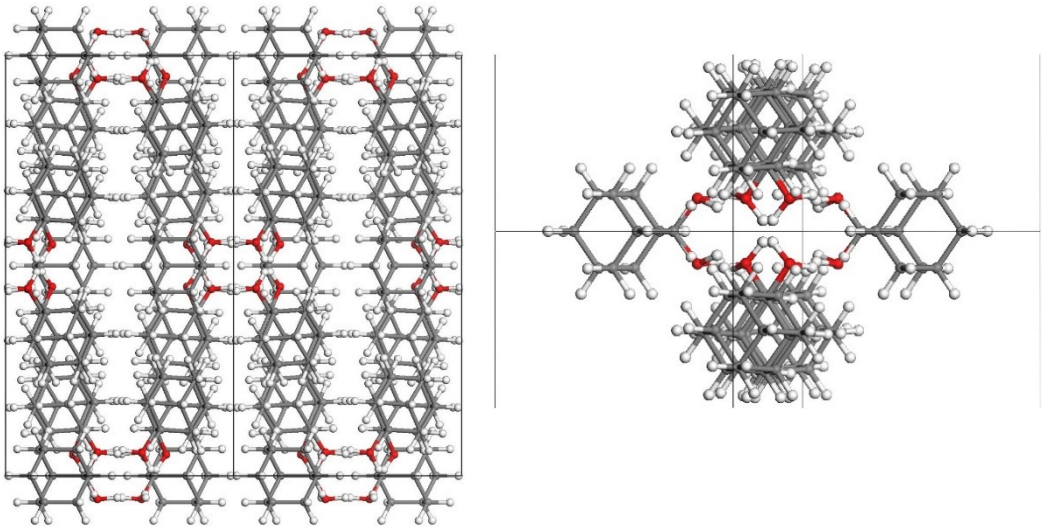

Figure S4c. Projections of the structure of the monoclinic C2/m phase II of 2-adamantanol at 330 K along the *c* plane (left panel) and on the *ac* plane.

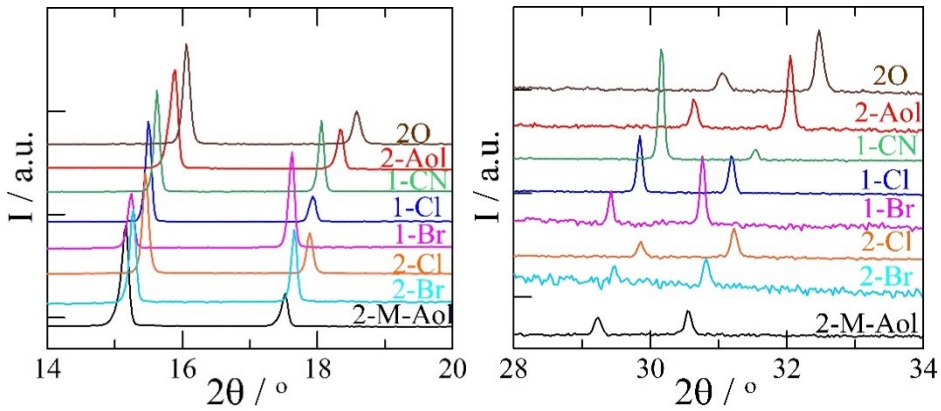

Figure S5a. Powder X-ray diffraction patterns of several 1-X- and 2-X-adamantane derivatives for the orientationally disordered phases for two different 2-theta windows. 1-Cl-adamanane (dark blue); 1-Br-adamantane (pink); 1-CN-adamantane (light green); 2-adamantanone (brown); 2-Cl-adamantane (orange); 2-Br-adamantane (light blue); 2-adamantanol (red); 2-methyl-2-adamantanol (black).

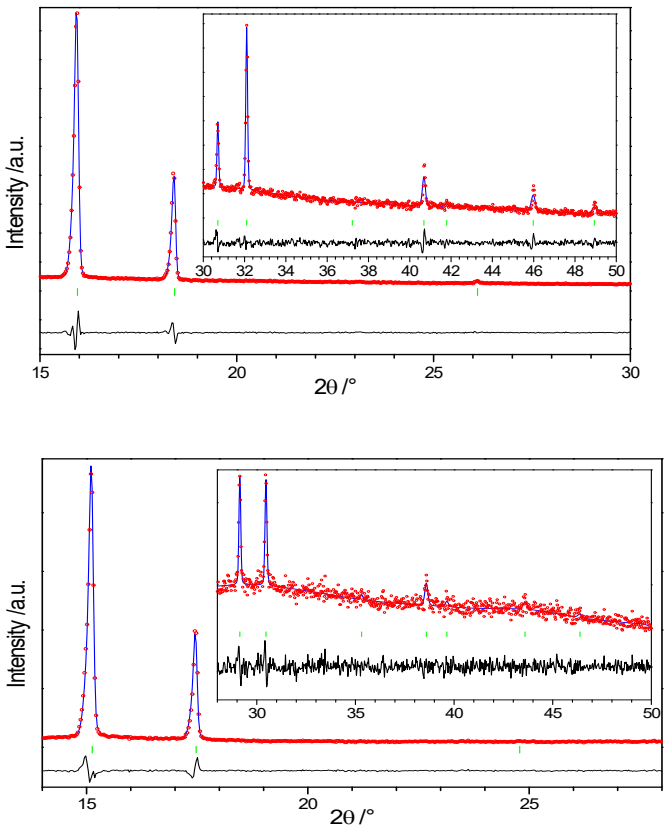

Figure S5b. Experimental (red circles) and Pawley refined (blue line) diffraction patterns along with difference profile (black line) and Bragg reflections (vertical green sticks) of the $Fm\bar{3}m$ space group phases I of 2-adamantanol at 401 K (top panel) and 2-methyl-2-adamantanol at 400 K (bottom panel). Insets correspond to the intensity scale magnified 20 times (2-adamantanol) and 12 times (2-methyl-2-adamantanol.

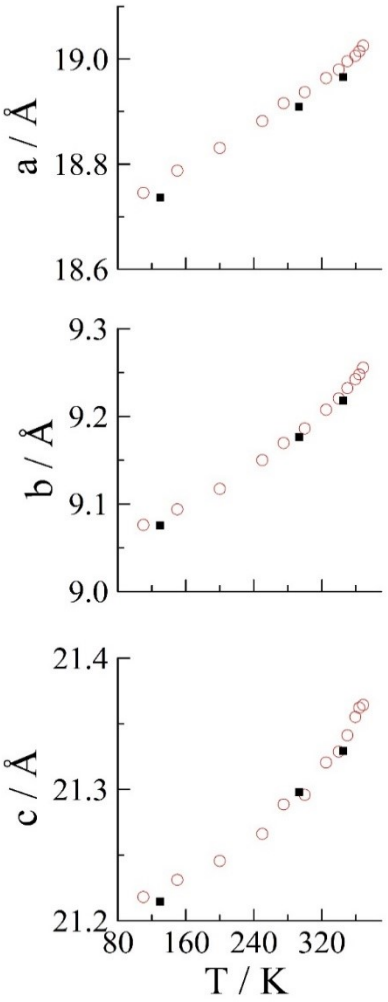

Figure S6. Lattice parameters as function of temperature for phase II of 2-methyl-2-adamantanol. Empty symbols correspond to power X-ray diffraction and full symbols to single-crystal X-ray diffraction.

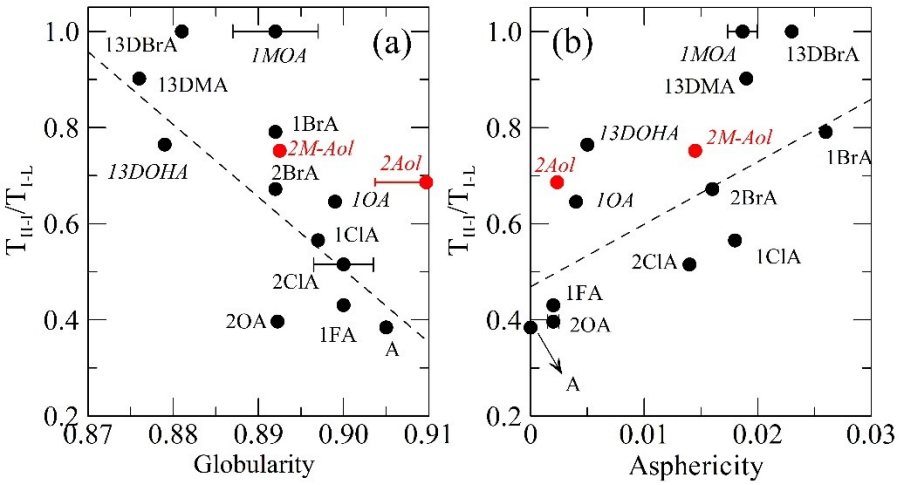

Figure S7. Ratio between the solid to plastic phase transition temperatures ($T_{II–I}$) and the melting temperatures ($T_{I–L}$) as a function of the globularity (a) and asphericity (b) parameters as derived from the Hirshfeld analysis of the low-temperature phases for some adamantane derivatives. Values are gathered in Table S2. Red points correspond to the compounds analyzed in this work, whereas black points were obtained from our previous work [2]. Horizontal bars show the dispersion due to the different values of the independent molecules of the asymmetric unit.

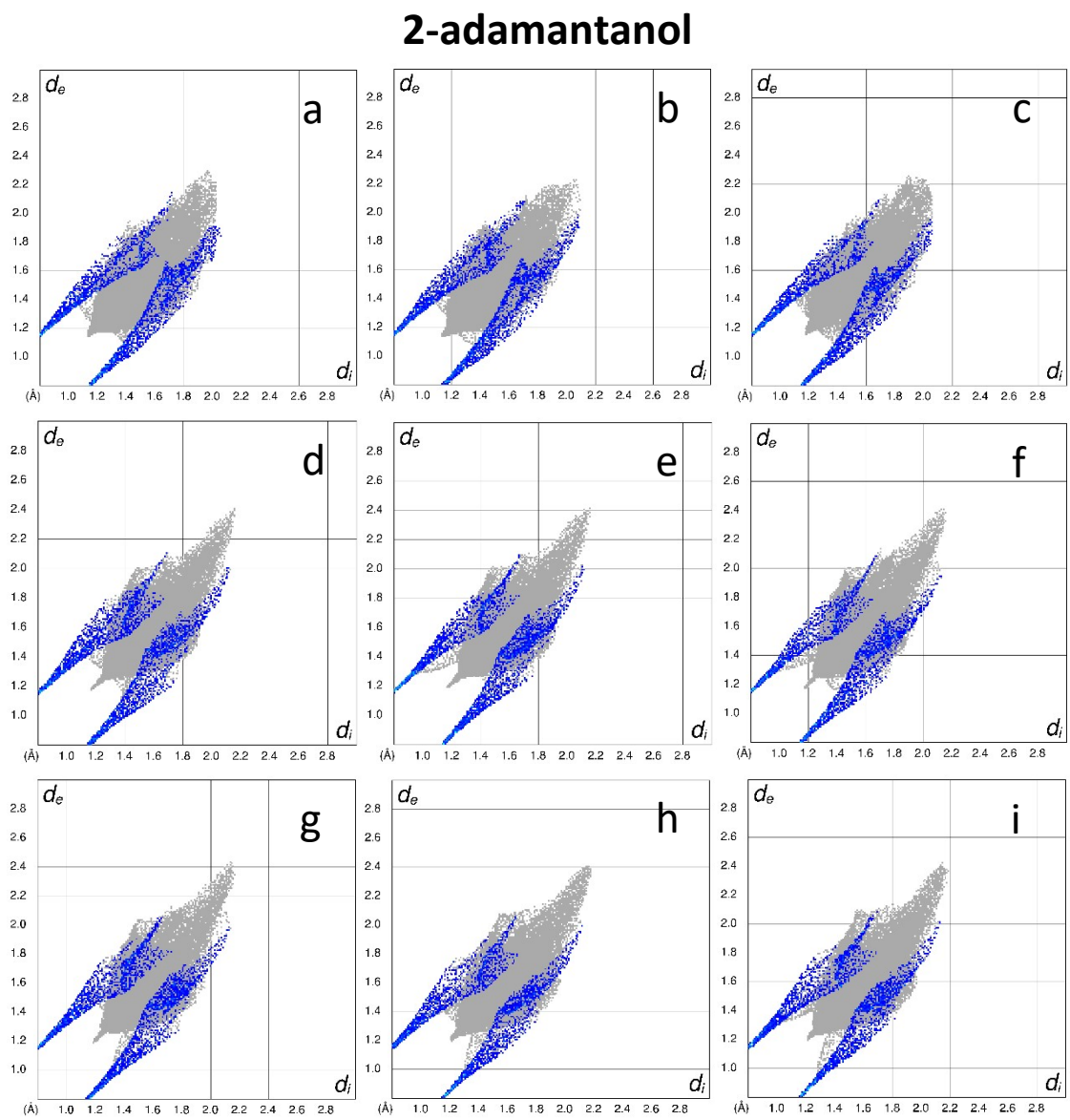

Figure S8a. Fingerprint plot O···H contacts of 2-adamantanol at 150 K phase IV for the 3 independent molecules (panels a, b, c), at 293 K, phase III, for the 6 different contacts (3 independent molecules and 2 occupation sites for the O atom) (panels d, e, f, g, h, i).

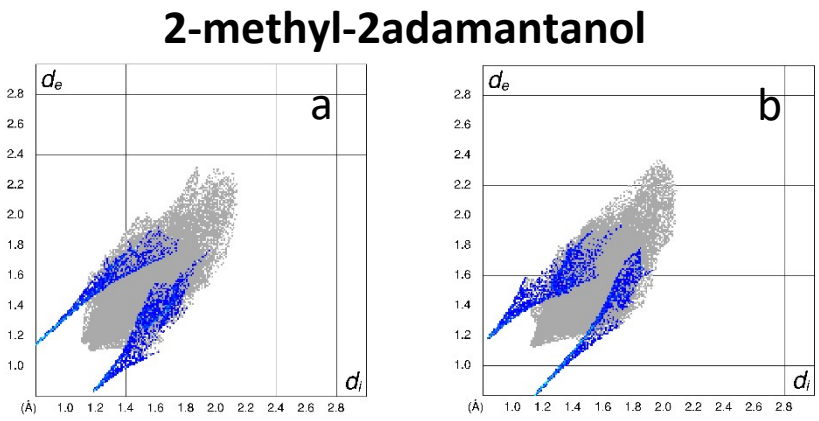

Figure S8b. Fingerprint plot O···H contacts of 2-methyl-2-adamantanol at 293 K phase II for the 2 independent molecules.

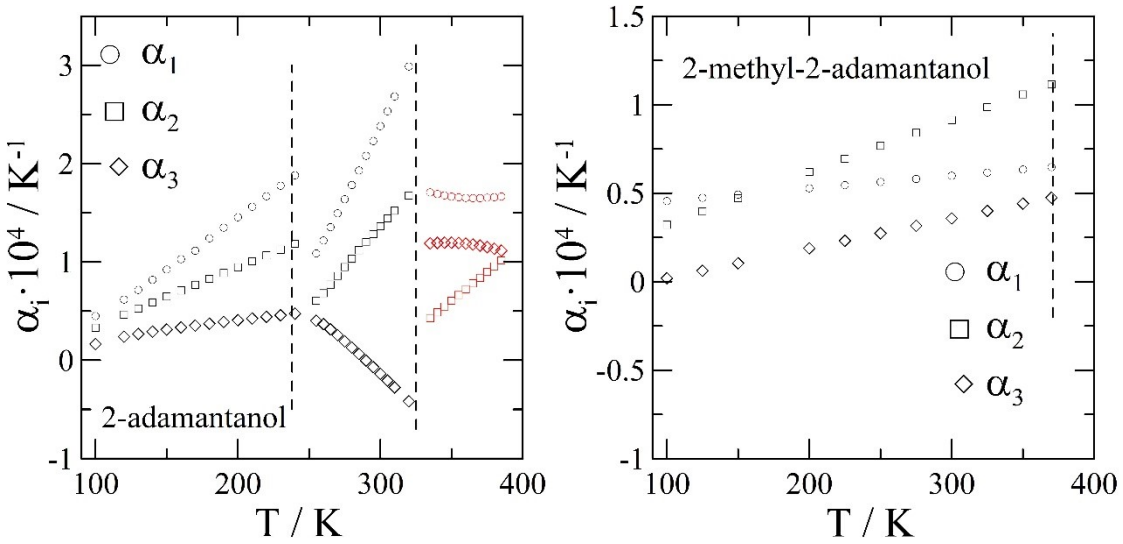

Figure S9. α_i eigenvalues of the thermal-expansion tensor as a function of temperature for phases IV, III and II (left panel) of 2-adamantanol and phase II for 2-methyl-2-adamantanol (right panel). Vertical dashed lines indicate the transition temperatures according to references [3,4].

References

[1] W. A. Dollase, Correction of Intensities for Preferred Orientation in Powder Diffractometry: Application of the March model. *J. Appl. Crystallogr.* 1986, **19**, 267–272

[2] Ph. Negrier, B. Ben Hassine, M. Barrio, M. Romanini, D. Mondieig, J.Ll. Tamarit, Polymorphism of 1,3-X-adamantanes (X = Br, OH, CH_3) and the crystal plastic phase formation ability, *CrystEngComm,* 2020, **22**, 1230-1238.

[3] M.B. Charapennikau, A.V. Blokhin, A.G. Kabo, G.J. Kabo, The heat capacities and parameters of solid phase transitions and fusion for 1- and 2-adamantanols, *J. Chem. Thermodynamics* 2003, **35**, 145–157.

[4] M.B. Charapennikau, A.V. Blokhin, G.J. Kabo*, A.G. Kabo, V.V. Diky, A.G. Gusakov, Thermodynamic properties and the plastic crystal state of 2-methyl-2-adamantanol, *Thermochim. Acta* 2002, **382**, 109–118.